Measurement of the Top Quark Mass in the All-Hadronic Mode at CDF

T. Aaltonen,[21] B. Álvarez González[z],[9] S. Amerio,[40] D. Amidei,[32] A. Anastassov[x],[15] A. Annovi,[17] J. Antos,[12] G. Apollinari,[15] J.A. Appel,[15] T. Arisawa,[54] A. Artikov,[13] J. Asaadi,[49] W. Ashmanskas,[15] B. Auerbach,[57] A. Aurisano,[49] F. Azfar,[39] W. Badgett,[15] T. Bae,[25] A. Barbaro-Galtieri,[26] V.E. Barnes,[44] B.A. Barnett,[23] P. Barria[hh],[42] P. Bartos,[12] M. Bauce[ff],[40] F. Bedeschi,[42] S. Behari,[23] G. Bellettini[gg],[42] J. Bellinger,[56] D. Benjamin,[14] A. Beretvas,[15] A. Bhatti,[46] D. Bisello[ff],[40] I. Bizjak,[28] K.R. Bland,[5] B. Blumenfeld,[23] A. Bocci,[14] A. Bodek,[45] D. Bortoletto,[44] J. Boudreau,[43] A. Boveia,[11] L. Brigliadori[ee],[6] C. Bromberg,[33] E. Brucken,[21] J. Budagov,[13] H.S. Budd,[45] K. Burkett,[15] G. Busetto[ff],[40] P. Bussey,[19] A. Buzatu,[31] A. Calamba,[10] C. Calancha,[29] S. Camarda,[4] M. Campanelli,[28] M. Campbell,[32] F. Canelli[11],[15] B. Carls,[22] D. Carlsmith,[56] R. Carosi,[42] S. Carrillo[m],[16] S. Carron,[15] B. Casal[k],[9] M. Casarsa,[50] A. Castro[ee],[6] P. Catastini,[20] D. Cauz,[50] V. Cavaliere,[22] M. Cavalli-Sforza,[4] A. Cerri[f],[26] L. Cerrito[s],[28] Y.C. Chen,[1] M. Chertok,[7] G. Chiarelli,[42] G. Chlachidze,[15] F. Chlebana,[15] K. Cho,[25] D. Chokheli,[13] W.H. Chung,[56] Y.S. Chung,[45] M.A. Ciocci[hh],[42] A. Clark,[18] C. Clarke,[55] G. Compostella[ff],[40] M.E. Convery,[15] J. Conway,[7] M.Corbo,[15] M. Cordelli,[17] C.A. Cox,[7] D.J. Cox,[7] F. Crescioli[gg],[42] J. Cuevas[z],[9] R. Culbertson,[15] D. Dagenhart,[15] N. d'Ascenzo[w],[15] M. Datta,[15] P. de Barbaro,[45] M. Dell'Orso[gg],[42] L. Demortier,[46] M. Deninno,[6] F. Devoto,[21] M. d'Errico[ff],[40] A. Di Canto[gg],[42] B. Di Ruzza,[15] J.R. Dittmann,[5] M. D'Onofrio,[27] S. Donati[gg],[42] P. Dong,[15] M. Dorigo,[50] T. Dorigo,[40] K. Ebina,[54] A. Elagin,[49] A. Eppig,[32] R. Erbacher,[7] S. Errede,[22] N. Ershaidat[dd],[15] R. Eusebi,[49] S. Farrington,[39] M. Feindt,[24] J.P. Fernandez,[29] R. Field,[16] G. Flanagan[u],[15] R. Forrest,[7] M.J. Frank,[5] M. Franklin,[20] J.C. Freeman,[15] Y. Funakoshi,[54] I. Furic,[16] M. Gallinaro,[46] J.E. Garcia,[18] A.F. Garfinkel,[44] P. Garosi[hh],[42] H. Gerberich,[22] E. Gerchtein,[15] S. Giagu,[47] V. Giakoumopoulou,[3] P. Giannetti,[42] K. Gibson,[43] C.M. Ginsburg,[15] N. Giokaris,[3] P. Giromini,[17] G. Giurgiu,[23] V. Glagolev,[13] D. Glenzinski,[15] M. Gold,[35] D. Goldin,[49] N. Goldschmidt,[16] A. Golossanov,[15] G. Gomez,[9] G. Gomez-Ceballos,[30] M. Goncharov,[30] O. González,[29] I. Gorelov,[35] A.T. Goshaw,[14] K. Goulianos,[46] S. Grinstein,[4] C. Grosso-Pilcher,[11] R.C. Group[53],[15] J. Guimaraes da Costa,[20] S.R. Hahn,[15] E. Halkiadakis,[48] A. Hamaguchi,[38] J.Y. Han,[45] F. Happacher,[17] K. Hara,[51] D. Hare,[48] M. Hare,[52] R.F. Harr,[55] K. Hatakeyama,[5] C. Hays,[39] M. Heck,[24] J. Heinrich,[41] M. Herndon,[56] S. Hewamanage,[5] A. Hocker,[15] W. Hopkins[g],[15] D. Horn,[24] S. Hou,[1] R.E. Hughes,[36] M. Hurwitz,[11] U. Husemann,[57] N. Hussain,[31] M. Hussein,[33] J. Huston,[33] G. Introzzi,[42] M. Iori[jj],[47] A. Ivanov[p],[7] E. James,[15] D. Jang,[10] B. Jayatilaka,[14] E.J. Jeon,[25] S. Jindariani,[15] M. Jones,[44] K.K. Joo,[25] S.Y. Jun,[10] T.R. Junk,[15] T. Kamon[25],[49] P.E. Karchin,[55] A. Kasmi,[5] Y. Kato[o],[38] W. Ketchum,[11] J. Keung,[41] V. Khotilovich,[49] B. Kilminster,[15] D.H. Kim,[25] H.S. Kim,[25] J.E. Kim,[25] M.J. Kim,[17] S.B. Kim,[25] S.H. Kim,[51] Y.K. Kim,[11] Y.J. Kim,[25] N. Kimura,[54] M. Kirby,[15] S. Klimenko,[16] K. Knoepfel,[15] K. Kondo*,[54] D.J. Kong,[25] J. Konigsberg,[16] A.V. Kotwal,[14] M. Kreps,[24] J. Kroll,[41] D. Krop,[11] M. Kruse,[14] V. Krutelyov[c],[49] T. Kuhr,[24] M. Kurata,[51] S. Kwang,[11] A.T. Laasanen,[44] S. Lami,[42] S. Lammel,[15] M. Lancaster,[28] R.L. Lander,[7] K. Lannon[y],[36] A. Lath,[48] G. Latino[hh],[42] T. LeCompte,[2] E. Lee,[49] H.S. Lee[q],[11] J.S. Lee,[25] S.W. Lee[bb],[49] S. Leo[gg],[42] S. Leone,[42] J.D. Lewis,[15] A. Limosani[t],[14] C.-J. Lin,[26] M. Lindgren,[15] E. Lipeles,[41] A. Lister,[18] D.O. Litvintsev,[15] C. Liu,[43] H. Liu,[53] Q. Liu,[44] T. Liu,[15] S. Lockwitz,[57] A. Loginov,[57] D. Lucchesi[ff],[40] J. Lueck,[24] P. Lujan,[26] P. Lukens,[15] G. Lungu,[46] J. Lys,[26] R. Lysak[e],[12] R. Madrak,[15] K. Maeshima,[15] P. Maestro[hh],[42] S. Malik,[46] G. Manca[a],[27] A. Manousakis-Katsikakis,[3] F. Margaroli,[47] C. Marino,[24] M. Martínez,[4] P. Mastrandrea,[47] K. Matera,[22] M.E. Mattson,[55] A. Mazzacane,[15] P. Mazzanti,[6] K.S. McFarland,[45] P. McIntyre,[49] R. McNulty[j],[27] A. Mehta,[27] P. Mehtala,[21] C. Mesropian,[46] T. Miao,[15] D. Mietlicki,[32] A. Mitra,[1] H. Miyake,[51] S. Moed,[15] N. Moggi,[6] M.N. Mondragon[m],[15] C.S. Moon,[25] R. Moore,[15] M.J. Morello[ii],[42] J. Morlock,[24] P. Movilla Fernandez,[15] A. Mukherjee,[15] Th. Muller,[24] P. Murat,[15] M. Mussini[ee],[6] J. Nachtman[n],[15] Y. Nagai,[51] J. Naganoma,[54] I. Nakano,[37] A. Napier,[52] J. Nett,[49] C. Neu,[53] M.S. Neubauer,[22] J. Nielsen[d],[26] L. Nodulman,[2] S.Y. Noh,[25] O. Norniella,[22] L. Oakes,[39] S.H. Oh,[14] Y.D. Oh,[25] I. Oksuzian,[53] T. Okusawa,[38] R. Orava,[21] L. Ortolan,[4] S. Pagan Griso[ff],[40] C. Pagliarone,[50] E. Palencia[f],[9] V. Papadimitriou,[15] A.A. Paramonov,[2] J. Patrick,[15] G. Pauletta[kk],[50] M. Paulini,[10] C. Paus,[30] D.E. Pellett,[7] A. Penzo,[50] T.J. Phillips,[14] G. Piacentino,[42] E. Pianori,[41] J. Pilot,[36] K. Pitts,[22] C. Plager,[8] L. Pondrom,[56] S. Poprocki[g],[15] K. Potamianos,[44] F. Prokoshin[cc],[13] A. Pranko,[26] F. Ptohos[h],[17] G. Punzi[gg],[42] A. Rahaman,[43] V. Ramakrishnan,[56] N. Ranjan,[44]

I. Redondo,[29] P. Renton,[39] M. Rescigno,[47] T. Riddick,[28] F. Rimondi[ee],[6] L. Ristori[42],[15] A. Robson,[19] T. Rodrigo,[9] T. Rodriguez,[41] E. Rogers,[22] S. Rolli[i],[52] R. Roser,[15] F. Ruffini[hh],[42] A. Ruiz,[9] J. Russ,[10] V. Rusu,[15] A. Safonov,[49] W.K. Sakumoto,[45] Y. Sakurai,[54] L. Santi[kk],[50] K. Sato,[51] V. Saveliev[w],[15] A. Savoy-Navarro[aa],[15] P. Schlabach,[15] A. Schmidt,[24] E.E. Schmidt,[15] T. Schwarz,[15] L. Scodellaro,[9] A. Scribano[hh],[42] F. Scuri,[42] S. Seidel,[35] Y. Seiya,[38] A. Semenov,[13] F. Sforza[hh],[42] S.Z. Shalhout,[7] T. Shears,[27] P.F. Shepard,[43] M. Shimojima[v],[51] M. Shochet,[11] I. Shreyber-Tecker,[34] A. Simonenko,[13] P. Sinervo,[31] K. Sliwa,[52] J.R. Smith,[7] F.D. Snider,[15] A. Soha,[15] V. Sorin,[4] H. Song,[43] P. Squillacioti[hh],[42] M. Stancari,[15] R. St. Denis,[19] B. Stelzer,[31] O. Stelzer-Chilton,[31] D. Stentz[x],[15] J. Strologas,[35] G.L. Strycker,[32] Y. Sudo,[51] A. Sukhanov,[15] I. Suslov,[13] K. Takemasa,[51] Y. Takeuchi,[51] J. Tang,[11] M. Tecchio,[32] P.K. Teng,[1] J. Thom[g],[15] J. Thome,[10] G.A. Thompson,[22] E. Thomson,[41] D. Toback,[49] S. Tokar,[12] K. Tollefson,[33] T. Tomura,[51] D. Tonelli,[15] S. Torre,[17] D. Torretta,[15] P. Totaro,[40] M. Trovato[ii],[42] F. Ukegawa,[51] S. Uozumi,[25] A. Varganov,[32] F. Vázquez[m],[16] G. Velev,[15] C. Vellidis,[15] M. Vidal,[44] I. Vila,[9] R. Vilar,[9] J. Vizán,[9] M. Vogel,[35] G. Volpi,[17] P. Wagner,[41] R.L. Wagner,[15] T. Wakisaka,[38] R. Wallny,[8] S.M. Wang,[1] A. Warburton,[31] D. Waters,[28] W.C. Wester III,[15] D. Whiteson[b],[41] A.B. Wicklund,[2] E. Wicklund,[15] S. Wilbur,[11] F. Wick,[24] H.H. Williams,[41] J.S. Wilson,[36] P. Wilson,[15] B.L. Winer,[36] P. Wittich[g],[15] S. Wolbers,[15] H. Wolfe,[36] T. Wright,[32] X. Wu,[18] Z. Wu,[5] K. Yamamoto,[38] D. Yamato,[38] T. Yang,[15] U.K. Yang[r],[11] Y.C. Yang,[25] W.-M. Yao,[26] G.P. Yeh,[15] K. Yi[n],[15] J. Yoh,[15] K. Yorita,[54] T. Yoshida[l],[38] G.B. Yu,[14] I. Yu,[25] S.S. Yu,[15] J.C. Yun,[15] A. Zanetti,[50] Y. Zeng,[14] C. Zhou,[14] and S. Zucchelli[ee]6

(CDF Collaboration[†])

[1]*Institute of Physics, Academia Sinica, Taipei, Taiwan 11529, Republic of China*
[2]*Argonne National Laboratory, Argonne, Illinois 60439, USA*
[3]*University of Athens, 157 71 Athens, Greece*
[4]*Institut de Fisica d'Altes Energies, ICREA, Universitat Autonoma de Barcelona, E-08193, Bellaterra (Barcelona), Spain*
[5]*Baylor University, Waco, Texas 76798, USA*
[6]*Istituto Nazionale di Fisica Nucleare Bologna,*
[ee]*University of Bologna, I-40127 Bologna, Italy*
[7]*University of California, Davis, Davis, California 95616, USA*
[8]*University of California, Los Angeles, Los Angeles, California 90024, USA*
[9]*Instituto de Fisica de Cantabria, CSIC-University of Cantabria, 39005 Santander, Spain*
[10]*Carnegie Mellon University, Pittsburgh, Pennsylvania 15213, USA*
[11]*Enrico Fermi Institute, University of Chicago, Chicago, Illinois 60637, USA*
[12]*Comenius University, 842 48 Bratislava, Slovakia; Institute of Experimental Physics, 040 01 Kosice, Slovakia*
[13]*Joint Institute for Nuclear Research, RU-141980 Dubna, Russia*
[14]*Duke University, Durham, North Carolina 27708, USA*
[15]*Fermi National Accelerator Laboratory, Batavia, Illinois 60510, USA*
[16]*University of Florida, Gainesville, Florida 32611, USA*
[17]*Laboratori Nazionali di Frascati, Istituto Nazionale di Fisica Nucleare, I-00044 Frascati, Italy*
[18]*University of Geneva, CH-1211 Geneva 4, Switzerland*
[19]*Glasgow University, Glasgow G12 8QQ, United Kingdom*
[20]*Harvard University, Cambridge, Massachusetts 02138, USA*
[21]*Division of High Energy Physics, Department of Physics,*
University of Helsinki and Helsinki Institute of Physics, FIN-00014, Helsinki, Finland
[22]*University of Illinois, Urbana, Illinois 61801, USA*
[23]*The Johns Hopkins University, Baltimore, Maryland 21218, USA*
[24]*Institut für Experimentelle Kernphysik, Karlsruhe Institute of Technology, D-76131 Karlsruhe, Germany*
[25]*Center for High Energy Physics: Kyungpook National University,*
Daegu 702-701, Korea; Seoul National University, Seoul 151-742,
Korea; Sungkyunkwan University, Suwon 440-746,
Korea; Korea Institute of Science and Technology Information,
Daejeon 305-806, Korea; Chonnam National University, Gwangju 500-757,
Korea; Chonbuk National University, Jeonju 561-756, Korea
[26]*Ernest Orlando Lawrence Berkeley National Laboratory, Berkeley, California 94720, USA*
[27]*University of Liverpool, Liverpool L69 7ZE, United Kingdom*
[28]*University College London, London WC1E 6BT, United Kingdom*
[29]*Centro de Investigaciones Energeticas Medioambientales y Tecnologicas, E-28040 Madrid, Spain*
[30]*Massachusetts Institute of Technology, Cambridge, Massachusetts 02139, USA*
[31]*Institute of Particle Physics: McGill University, Montréal,*
Québec, Canada H3A 2T8; Simon Fraser University, Burnaby,
British Columbia, Canada V5A 1S6; University of Toronto,
Toronto, Ontario, Canada M5S 1A7; and TRIUMF,
Vancouver, British Columbia, Canada V6T 2A3

[32] University of Michigan, Ann Arbor, Michigan 48109, USA
[33] Michigan State University, East Lansing, Michigan 48824, USA
[34] Institution for Theoretical and Experimental Physics, ITEP, Moscow 117259, Russia
[35] University of New Mexico, Albuquerque, New Mexico 87131, USA
[36] The Ohio State University, Columbus, Ohio 43210, USA
[37] Okayama University, Okayama 700-8530, Japan
[38] Osaka City University, Osaka 588, Japan
[39] University of Oxford, Oxford OX1 3RH, United Kingdom
[40] Istituto Nazionale di Fisica Nucleare, Sezione di Padova-Trento,
[ff] University of Padova, I-35131 Padova, Italy
[41] University of Pennsylvania, Philadelphia, Pennsylvania 19104, USA
[42] Istituto Nazionale di Fisica Nucleare Pisa, [gg] University of Pisa,
[hh] University of Siena and [ii] Scuola Normale Superiore, I-56127 Pisa, Italy
[43] University of Pittsburgh, Pittsburgh, Pennsylvania 15260, USA
[44] Purdue University, West Lafayette, Indiana 47907, USA
[45] University of Rochester, Rochester, New York 14627, USA
[46] The Rockefeller University, New York, New York 10065, USA
[47] Istituto Nazionale di Fisica Nucleare, Sezione di Roma 1,
[jj] Sapienza Università di Roma, I-00185 Roma, Italy
[48] Rutgers University, Piscataway, New Jersey 08855, USA
[49] Texas A&M University, College Station, Texas 77843, USA
[50] Istituto Nazionale di Fisica Nucleare Trieste/Udine,
I-34100 Trieste, [kk] University of Udine, I-33100 Udine, Italy
[51] University of Tsukuba, Tsukuba, Ibaraki 305, Japan
[52] Tufts University, Medford, Massachusetts 02155, USA
[53] University of Virginia, Charlottesville, Virginia 22906, USA
[54] Waseda University, Tokyo 169, Japan
[55] Wayne State University, Detroit, Michigan 48201, USA
[56] University of Wisconsin, Madison, Wisconsin 53706, USA
[57] Yale University, New Haven, Connecticut 06520, USA

We present a measurement of the top quark mass ($M_{\rm top}$) in the all-hadronic decay channel using 5.8 fb^{-1} of $p\bar{p}$ data collected with the CDF II detector at the Fermilab Tevatron Collider. Events with six to eight jets are selected by a neural network algorithm and by the requirement that at least one of the jets is tagged as a b quark jet. The measurement is performed by a likelihood fit technique, which simultaneously determines $M_{\rm top}$ and the jet energy scale (JES) calibration. The fit yields a value of $M_{\rm top} = 172.5 \ \pm 1.4\,({\rm stat}) \ \pm 1.0\,({\rm JES}) \ \pm 1.1\,({\rm syst})$ GeV/c^2.

PACS numbers: 14.65.Ha, 13.85.Ni,13.85.Qk

The mass of the top quark ($M_{\rm top}$) is a fundamental parameter of the standard model (SM), and its large value makes the top quark contribution dominant in loop corrections to many observables, like the W boson mass M_W. Precise measurements of M_W and $M_{\rm top}$ allow one to set indirect constraints on the mass of the, yet unobserved, Higgs boson [1].

In this Letter we present a measurement of $M_{\rm top}$ using proton-antiproton collision events at a center-of-mass energy of 1.96 TeV. Top quarks are produced mostly in pairs ($t\bar{t}$), with each top quark decaying immediately into a W boson and a b quark nearly 100% of the time, in the framework of the SM. In this analysis only events where both the W's decay to a quark-antiquark pair are considered. This all-hadronic final state has the advantage of being the decay channel with the largest branching ratio (46%), but it is overwhelmed by the QCD multijet background processes, which surpass $t\bar{t}$ production by three orders of magnitude even after a dedicated trigger requirement. Nevertheless, it will be shown how this difficult background can be succesfully controlled and signif-

*Deceased
†With visitors from [a]Istituto Nazionale di Fisica Nucleare, Sezione di Cagliari, 09042 Monserrato (Cagliari), Italy, [b]University of CA Irvine, Irvine, CA 92697, USA, [c]University of CA Santa Barbara, Santa Barbara, CA 93106, USA, [d]University of CA Santa Cruz, Santa Cruz, CA 95064, USA, [e]Institute of Physics, Academy of Sciences of the Czech Republic, Czech Republic, [f]CERN, CH-1211 Geneva, Switzerland, [g]Cornell University, Ithaca, NY 14853, USA, [h]University of Cyprus, Nicosia CY-1678, Cyprus, [i]Office of Science, U.S. Department of Energy, Washington, DC 20585, USA, [j]University College Dublin, Dublin 4, Ireland, [k]ETH, 8092 Zurich, Switzerland, [l]University of Fukui, Fukui City, Fukui Prefecture, Japan 910-0017, [m]Universidad Iberoamericana, Mexico D.F., Mexico, [n]University of Iowa, Iowa City, IA 52242, USA, [o]Kinki University, Higashi-Osaka City, Japan 577-8502, [p]Kansas State University, Manhattan, KS 66506, USA, [q]Korea University, Seoul, 136-713, Korea, [r]University of Manchester, Manchester M13 9PL, United Kingdom, [s]Queen Mary, University of London, London, E1 4NS, United Kingdom, [t]University of Melbourne, Victoria 3010, Australia, [u]Muons, Inc., Batavia, IL 60510, USA, [v]Nagasaki Institute of Applied Science, Nagasaki, Japan, [w]National Research Nuclear University, Moscow, Russia, [x]Northwestern University, Evanston, IL 60208, USA,
[y]University of Notre Dame, Notre Dame, IN 46556, USA, [z]Universidad de Oviedo, E-33007 Oviedo, Spain, [aa]CNRS-IN2P3, Paris, F-75205 France, [bb]Texas Tech University, Lubbock, TX 79609, USA, [cc]Universidad Tecnica Federico Santa Maria, 110v Valparaiso, Chile, [dd]Yarmouk University, Irbid 211-63, Jordan,

icantly suppressed with a properly optimized event selection. Comparing to the previous measurement in the same channel at CDF [2], the improvements in the analysis technique and a larger dataset allow us to decrease the total uncertainty on $M_{\rm top}$ by 21%. The additional dataset has been acquired at higher instantaneous luminosity, which results in higher number of background events in the data sample. Despite this fact, we managed to introduce significant improvements to the analysis and achieve the world best measurement of $M_{\rm top}$ in the all-hadronic channel so far, also entering with the third largest weight in the $M_{\rm top}$ world average calculation [3].

The data correspond to an integrated luminosity of $5.8\,{\rm fb}^{-1}$. They have been collected between March 2002 and February 2010 by the CDF detector, a general-purpose apparatus designed to study $p\bar{p}$ collisions at the Tevatron and described in detail in [4]. Events used in this measurement are selected by a multijet trigger requirement [2], and retained only if they are well contained in the detector acceptance, have no well identified energetic electron or muon, and have no significant missing transverse energy $\not\!\!E_T$ [5]. Candidate events are also required to have from six to eight "tight" ($E_T \geq 15\,{\rm GeV}$ and $|\eta| \leq 2.0$) jets. After this preselection, a total of about 5.6 M events is observed in the data, with less than 9 thousand expected from $t\bar{t}$ events. To improve the signal-to-background ratio (S/B) a multivariate algorithm is implemented. An artificial neural network, based on a set of kinematic and jet shape variables [2], is used to take advantage of the distinctive features of signal and background events. The neural network was trained using simulated $t\bar{t}$ events generated by PYTHIA [6] and propagated through the CDF detector simulation. At this level of the selection the fraction of signal events is still negligible and the data are used to represent the background. The value of the output node $N_{\rm out}$, is used as a discriminant between signal and background. In order to further increase the signal purity, a b-tagging algorithm [7] is used to identify ("b-tag" or simply "tag") jets that most likely resulted from the fragmentation of a b quark. Only events with one to three tagged jets are then retained.

The background for the $t\bar{t}$ multijet final state comes mainly from QCD production of heavy-quark pairs ($b\bar{b}$ and $c\bar{c}$) and events with false b-tags of light-quark and gluon jets. Given the large theoretical uncertainties on the QCD multijet production cross section, the background normalization is obtained from the data themselves. A tag rate per jet is used, defined as the probability of tagging a jet whose tracks are reconstructed in the tracking system ("fiducial" jet). This rate is evaluated from events passing the preselection with five tight jets ($S/B \approx 1/2000$), and it is parametrized in terms of the jet E_T, the number of tracks associated to the jet, and the number of primary vertices reconstructed in the event. The rate of a fiducial jet in a candidate event selected before the b-tagging represents an estimate of the probability for that jet to come from background and to be tagged. This allows one to predict the number of background events with a given number of tagged jets as well as their distributions [2]. The background modeling is tested in background-dominated control regions with six to eight jets and small values of N_{out}. Small residual discrepancies are accounted for as systematic uncertainties.

This analysis employs the template method to measure $M_{\rm top}$ with simultaneous calibration of the jet energy scale (JES). The latter is a multiplicative factor representing a correction applied to the raw energy of a reconstructed jet ($E_T^{\rm raw}$), so that the its corrected energy $E_T = {\rm JES} \cdot E_T^{\rm raw}$, is a better estimate of the energy of the underlying parton [8]. Discrepancies between data and simulation lead to an uncertainty on the JES used in Monte Carlo (MC) events, and, as a consequence, on the measurements of $M_{\rm top}$. The MC distributions of the reconstructed top quark mass, $m_t^{\rm rec}$, and W boson mass, $m_W^{\rm rec}$, are used as a reference ("template") in the measurement, with the latter providing the information necessary to calibrate "in situ" the JES, by using the precisely measured value of the W boson mass [9].

For each selected event, the six highest-E_T jets are assumed to come from the quarks of a $t\bar{t}$ all-hadronic final state. Each of the different combinations where the jets are arranged in two doublets (the W bosons) and two triplets (the top quarks) is considered. To reduce the number of permutations, b-tagged jets are assumed to come from b quarks only resulting in 30, 6 or 18 permutations for events with one, two or three tagged jets, respectively [10]. For each permutation $m_t^{\rm rec}$ is obtained through a constrained fit based on the minimization of the following χ^2-like function:

$$\begin{aligned}\chi^2_t \;=\; & \frac{\left(m^{(1)}_{jj} - M_W\right)^2}{\Gamma^2_W} + \frac{\left(m^{(2)}_{jj} - M_W\right)^2}{\Gamma^2_W} \\ & + \frac{\left(m^{(1)}_{jjb} - m_t^{\rm rec}\right)^2}{\Gamma^2_t} + \frac{\left(m^{(2)}_{jjb} - m_t^{\rm rec}\right)^2}{\Gamma^2_t} \\ & + \sum_{i=1}^{6} \frac{\left(p^{\rm fit}_{T,i} - p^{\rm meas}_{T,i}\right)^2}{\sigma_i^2}\end{aligned}$$

where $m_{jj}^{(1,2)}$ are the invariant masses of the two pairs of jets assigned to light flavor quarks, $m_{jjb}^{(1,2)}$ are the invariant masses of the triplets including one pair and a b-tagged jet, $M_W = 80.4\,{\rm GeV}/c^2$ and $\Gamma_W = 2.1\,{\rm GeV}/c^2$ are the measured mass and natural width of the W boson [9], and $\Gamma_t = 1.5\,{\rm GeV}/c^2$ is the assumed natural width of the top quark [11]. The jet transverse momenta are constrained in the fit to the measured values, $p_{T,i}^{\rm meas}$, within their known resolutions, σ_i. The fit is performed with respect to $m_t^{\rm rec}$ and the transverse momenta of the jets $p_{T,i}^{\rm fit}$, and the permutation which gives the lowest value for the minimized χ^2_t is

selected. The variable $m_W^{\rm rec}$ is reconstructed by the same procedure considered for $m_t^{\rm rec}$, but with a χ^2 function, χ^2_W, where also the W mass is left free to vary in the fit. The selected values of $m_t^{\rm rec}$ and $m_W^{\rm rec}$ enter the respective distributions, built separately for events with exactly one or ≥ 2 tags [12].

Signal templates are built using MC events with $M_{\rm top}$ values from 160 to 185 GeV/c^2, with steps of 2.5 GeV/c^2. For each $M_{\rm top}$ the corrected jets' E_T are changed to values E'_T given by $E'_T = [1 + \Delta{\rm JES} \cdot (\sigma_{\rm JES}/{\rm JES})] \cdot E_T$, where $\sigma_{\rm JES}$ is the absolute uncertainty on the JES and ΔJES is a dimensionless number. This equivalently means that the applied JES differs by $\Delta{\rm JES} \times \sigma_{\rm JES}$ from the default value. To be noted that $\sigma_{\rm JES}/{\rm JES}$ is a function of the jet E_T [8]. Values of ΔJES between -2 and $+2$, in steps of 0.5, have been considered, and in the following we refer to this parameter to denote variations of the JES.

To construct the background templates we apply the fitting technique to the data events passing the neural network selection cut, omitting the b-tagging requirement ("pretag" sample). All possible combinations are considered where one to three fiducial jets are treated as tagged. The weight of each combination is given by the probability, evaluated by the tag rates, that those jets are tagged in the event by the b-tagging algorithm, and it is used for the corresponding values of $m_t^{\rm rec}$ and $m_W^{\rm rec}$ to build the templates. As the procedure is applied to data, signal contributions must be properly subtracted.

Sets of simulated experiments ("pseudo-experiments", PEs) have been performed to optimize the requirements on the values of $N_{\rm out}$, χ^2_t and χ^2_W in order to minimize the statistical uncertainty on the $M_{\rm top}$ measurement. As an improvement with respect to [2], two different sets of events, denoted by $S_{\rm JES}$ and $S_{M_{\rm top}}$, are considered to build the $m_W^{\rm rec}$ and $m_t^{\rm rec}$ templates, respectively. This choice contributes in reducing the final total uncertainty on $M_{\rm top}$ with respect to [2] by about 12%. The set $S_{\rm JES}$ is selected by using cuts on $N_{\rm out}$ and χ^2_W, while $S_{M_{\rm top}}$ is selected by a further requirement on χ^2_t, so that $S_{M_{\rm top}} \subseteq S_{\rm JES}$. The procedure gives $\{N_{\rm out} \geq 0.97,\, \chi^2_W \leq 2,\, \chi^2_t \leq 3\}$ and $\{N_{\rm out} \geq 0.94,\, \chi^2_W \leq 3,\, \chi^2_t \leq 4\}$ as the optimized selection requirements for 1-tag and $\geq$ 2-tag events respectively. Correlations between $m_t^{\rm rec}$ and $m_W^{\rm rec}$ in events selected both in $S_{M_{\rm top}}$ and in $S_{\rm JES}$ are taken into account during the calibration procedure described below.

In order to measure $M_{\rm top}$ simultaneously with JES, a fit is performed in which an unbinned extended likelihood function is maximized to find the values of $M_{\rm top}$, ΔJES, and the number of signal (n_s) and background (n_b) events for each tagging category which best reproduce the observed distributions of $m_t^{\rm rec}$ and $m_W^{\rm rec}$. The likelihood depends on the probability density functions (p.d.f.'s) expected for signal (s) and background (b): $P_{\rm s}\,(m_t^{\rm rec}|\,M_{\rm top},\,\Delta{\rm JES})$, $P_{\rm s}\,(m_W^{\rm rec}|\,M_{\rm top},\,\Delta{\rm JES})$, $P_{\rm b}\,(m_t^{\rm rec})$, and $P_{\rm b}\,(m_W^{\rm rec})$. The p.d.f.'s are obtained by fitting normalized functions to the templates, initially built as histograms. For the signal the continuous dependence of the p.d.f.'s on $M_{\rm top}$ and ΔJES is obtained by fitting simultaneously the whole set of templates, corresponding to the large set of values simulated for those two variables. In the fit a linear dependence of the parameters of the p.d.f.'s on $M_{\rm top}$ and ΔJES is assumed, so that the resulting fitted functions have continuous variable shapes [2]. Figure 1 shows examples of signal and background templates for the $\geq$ 2-tag sample, with the corresponding p.d.f.'s superimposed.

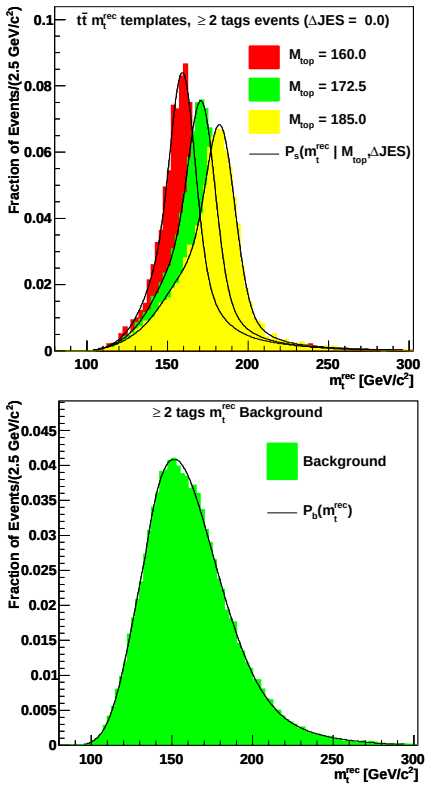

FIG. 1: Templates of $m_t^{\rm rec}$ for events with $\geq$ 2 tags and corresponding probability density functions superimposed. Top plot: the signal p.d.f, $P_{\rm s}$, for various values of $M_{\rm top}$ and $\Delta{\rm JES} = 0$. Bottom plot: the background p.d.f., $P_{\rm b}$.

The likelihood function used for the measurement can be divided into three parts:

$$\mathcal{L} = \mathcal{L}_{1\,\rm tag} \times \mathcal{L}_{\geq 2\,\rm tags} \times \mathcal{L}_{\Delta{\rm JES}_{\rm constr}}$$

where $\mathcal{L}_{\Delta{\rm JES}_{\rm constr}}$ is a gaussian term constraining the JES to the nominal value (i.e. ΔJES to 0) within its uncertainty. Terms $\mathcal{L}_{1\,\rm tag}$ and $\mathcal{L}_{\geq 2\,\rm tags}$ are defined as:

$$\mathcal{L}_{1,\geq 2\,\rm tags} = \mathcal{L}_{\rm JES} \times \mathcal{L}_{M_{\rm top}} \times \mathcal{L}_{\rm evts} \times \mathcal{L}_{N^{\rm bkg}_{\rm constr}}\,,$$

where, omitting the dependences on $M_{\rm top}$ and $\Delta_{\rm JES}$,

$$\mathcal{L}_{\rm JES} = \prod_{i=1}^{N_{\rm obs}^{S_{\rm JES}}} \frac{n_s P_s^{m_W^{\rm rec}}\,(m_{W,\,i}) + n_b P_b^{m_W^{\rm rec}}\,(m_{W,\,i})}{n_s + n_b}$$

and

$$\mathcal{L}_{M_{\rm top}} = \prod_{i=1}^{N_{\rm obs}^{S_{M_{\rm top}}}} \frac{\mathcal{A}_s n_s P_s^{m_t^{\rm rec}}(m_{t,i}) + \mathcal{A}_b n_b P_b^{m_t^{\rm rec}}(m_{t,i})}{\mathcal{A}_s n_s + \mathcal{A}_b n_b} .$$

Here the probability of observing the $N_{\rm obs}^{S_{\rm JES}}$ values of $m_W^{\rm rec}$ and the $N_{\rm obs}^{S_{M_{\rm top}}}$ values of $m_t^{\rm rec}$ reconstructed in the data $S_{\rm JES}$ and $S_{M_{\rm top}}$ samples, respectively, is evaluated from the expected distributions as a function of the fit parameters $M_{\rm top}$, ΔJES, n_s, and n_b. The factors $\mathcal{A}_s$ and $\mathcal{A}_b$ represent the acceptance of $S_{M_{\rm top}}$ with respect to $S_{\rm JES}$ for signal and background, respectively (i.e., the fraction of events selected by the requirements on χ_t^2 only). For the signal this acceptance is parametrized as a function of the fit parameters $M_{\rm top}$ and ΔJES. The other two factors included in $\mathcal{L}_{1,\geq 2{\rm tags}}$ are: $\mathcal{L}_{\rm evts}$, which gives the probability of observing the number of events selected in the data, evaluated by Poisson and binomial distributions, and $\mathcal{L}_{N_{\rm constr}^{\rm bkg}}$ which constrains the parameter n_b to the *a priori* estimate of the expected background, obtained by the tag rate.

The possible presence of biases in the $M_{\rm top}$ and ΔJES values returned by the likelihood fit has been investigated. Pseudo-experiments are performed assuming specific values for $M_{\rm top}$ and ΔJES and "pseudo-data" are therefore extracted from the corresponding signal and background templates. The results of these PEs have been compared to the input values and calibration functions to be applied to the output from the fit have been defined in order to obtain, on average, a more reliable estimate of the true values and uncertainties.

Finally, the likelihood fit is applied to data. After the event selection described above, we are left with 4368 and 1196 events with one and $\geq$ 2 tags, respectively, in the $S_{\rm JES}$ sample. The corresponding expected numbers of background events amount to 3652 ± 181 and 718 ± 14. The tighter requirements used for the $S_{M_{\rm top}}$ samples select 2256 with one tag and 600 with ≥ 2 tags, with average background estimates of 1712 ± 77 and 305 ± 22, respectively.

For these events the variables $m_W^{\rm rec}$ and $m_t^{\rm rec}$ have been reconstructed and used as the data inputs to the likelihood fit. Once the calibration procedure has been applied, the measurements of $M_{\rm top}$ and ΔJES are

$$\begin{aligned} M_{\rm top} &= 172.5 \pm 1.4\,({\rm stat}) \pm 1.0\,({\rm JES})\ {\rm GeV}/c^2 \\ \Delta{\rm JES} &= -0.1 \pm 0.3\,({\rm stat}) \pm 0.3\,(M_{\rm top})\,. \end{aligned}$$

Figure 2 shows the measured values together with the negative log-likelihood contours whose projections correspond to one, two, and three σ uncertainties on the values of $M_{\rm top}$ and ΔJES.

Figure 3 shows the $m_t^{\rm rec}$ and $m_W^{\rm rec}$ distributions for the data compared to the expected background and the signal for $M_{\rm top}$ and ΔJES corresponding to the measured values. The signal and background distributions are normalized to the respective yields as fitted to the data, with the 1-tag and $\geq$ 2-tag contributions summed together.

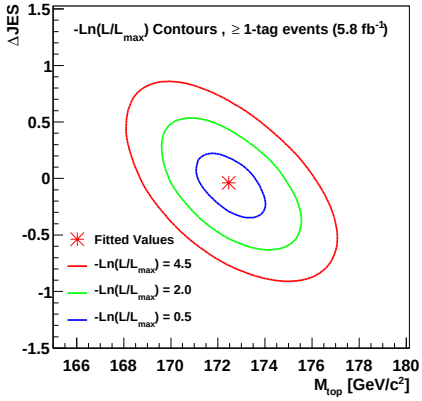

FIG. 2: Negative log-likelihood contours for the likelihood fit performed for the $M_{\rm top}$ and ΔJES measurement. The minimum is shown along with the contours whose projections correspond to one, two, and three σ uncertainties on the $M_{\rm top}$ and ΔJES measurements.

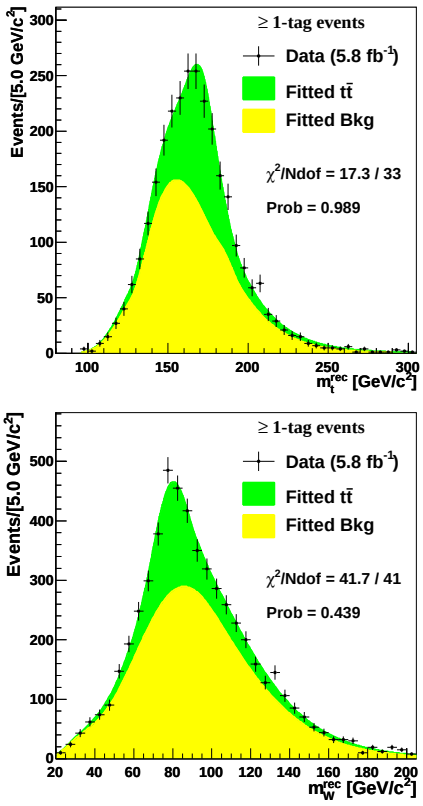

FIG. 3: Distributions of $m_t^{\rm rec}$ (top plot) and $m_W^{\rm rec}$ (bottom plot) as obtained in the selected data (black points) with $\geq$ 1 tags, compared to the distributions from signal and background corresponding to the measured values of $M_{\rm top}$ and ΔJES. The expected distributions are normalized to the best fit values for the average number of signal and background events.

Various sources of systematic uncertainties affect the $M_{\rm top}$ and JES measurements, as described in [2]. They are evaluated by performing PEs using templates built by signal samples where effects due to systematic uncertainties have been included. The differences in the average values of $M_{\rm top}$ and JES with respect to the PEs performed with default templates are then considered. Possible residual biases existing after the calibration, and uncertainties on the parameters of the calibration functions are also taken into account. The largest contributions come from uncertainties on the modeling of the background, on the simulation of $t\bar{t}$ events, and on the individual corrections which the JES depends on [8]. Table I shows a summary of all the systematic uncertainties.

TABLE I: Sources of systematic uncertainty affecting the $M_{\rm top}$ and ΔJES measurements. The total uncertainty is obtained by the quadrature sum of each contribution.

Source	$\delta M_{\rm top}$ (GeV/c^2)	$\delta\Delta$JES
Residual bias	0.2	0.03
Calibration	0.1	0.01
Generator	0.5	0.21
Initial / final state radiation	0.1	0.04
b-jet energy scale	0.2	0.05
b-tag	0.1	0.01
Residual JES	0.4	$--$
Parton distribution functions	0.2	0.04
Multiple $p\bar{p}$ interactions	0.1	0.04
Color reconnection	0.3	0.12
Statistics of templates	0.3	0.05
Background	0.6	0.11
Trigger	0.2	0.04
Total	1.1	0.29

In summary, we have presented a measurement of the top quark mass in the all-hadronic channel, using $5.8\,{\rm fb}^{-1}$ of $p\bar{p}$ collision data. The measured value is $M_{\rm top} = 172.5 \pm 1.4\,({\rm stat}) \pm 1.0\,({\rm JES}) \pm 1.1\,({\rm syst})$ GeV/c^2, for a total uncertainty of $2.0\,{\rm GeV}/c^2$. This result complements and is consistent with the most recent measurements obtained in the other channels by the CDF and D0 Collaborations, and also represents the only measurement in the all-hadronic channel for the Run II of the Tevatron [3].

We thank the Fermilab staff and the technical staffs of the participating institutions for their vital contributions. This work was supported by the U.S. Department of Energy and National Science Foundation; the Italian Istituto Nazionale di Fisica Nucleare; the Ministry of Education, Culture, Sports, Science and Technology of Japan; the Natural Sciences and Engineering Research Council of Canada; the National Science Council of the Republic of China; the Swiss National Science Foundation; the A.P. Sloan Foundation; the Bundesministerium für Bildung und Forschung, Germany; the Korean World Class University Program, the National Research Foundation of Korea; the Science and Technology Facilities Council and the Royal Society, UK; the Institut National de Physique Nucleaire et Physique des Particules/CNRS; the Russian Foundation for Basic Research; the Ministerio de Ciencia e Innovación, and Programa Consolider-Ingenio 2010, Spain; the Slovak R&D Agency; the Academy of Finland; and the Australian Research Council (ARC).

[1] The ALEPH, CDF, D0, DELPHI, L3, OPAL, SLD Collaborations, The LEP Electroweak Working Group, the Tevatron Electroweak Working Group, and the SLD electroweak and heavy flavour groups, *Precision Electroweak Measurements and Constraints on the Standard Model*, arXiv:1012.2367 (2010).

[2] T. Aaltonen *et al.* (CDF Collaboration), Phys. Rev. D **81** (2010) 052011.

[3] The Tevatron Electroweak Working Group for the CDF and D0 Collaborations, *Combination of CDF and D0 results on the mass of the top quark using up to* $5.8\,fb^{-1}$ *of data*, arXiv:1107.5255 [hep-ex] (2011).

[4] D. Acosta *et al.* (CDF Collaboration), Phys. Rev. D **71** (2005) 032001.

[5] We use a cylindrical coordinate system where θ is the polar angle with respect to the proton beam direction (z axis), ϕ is the azimuthal angle about the beam axis, and the pseudorapidity is defined as $\eta = -\ln\tan(\theta/2)$. A particle's transverse momentum p_T and tranverse energy E_T are given by $|p|\sin\theta$ and $E\sin\theta$ respectively. The missing E_T vector, $\vec{\not\!\!E}_T$, is defined by $\vec{\not\!\!E}_T = -\sum_i E_{T,i}\,\hat{n}_{T,i}$ where $\hat{n}_{T,i}$ is the unit vector in the $x-y$ plane pointing from the primary interaction vertex to a given calorimeter tower i, and $E_{T,i}$ is the E_T measured in that tower. Finally $\not\!\!E_T = |\vec{\not\!\!E}_T|$.

[6] T. Sjöstrand *et al.*, Comput. Phys. Commun. **135** (2001) 238.

[7] D. Acosta *et al.* (CDF Collaboration), Phys. Rev. D **71** (2005) 052003.

[8] A. Bhatti *et al.*, Nucl. Instrum. Methods Phys. Res., Sect. A **566** (2006) 375.

[9] K. Nakamura *et al.* (Particle Data Group), J. Phys. G **37**, 075021 (2010).

[10] If three b-tagged jets are present in the event, the three possible assignments of two out of three of them to b quarks are also considered, while the remaining

one is treated as a light flavor jet.

[11] S. M. Oliveira, L. Brucher, R. Santos and A. Barroso, Phys. Rev. D **64**, 017301 (2001).

[12] The notation "≥ 2" refers to events with two or three tagged jets.